THE UNIVERSITY *of* EDINBURGH

Edinburgh Research Explorer

The Punching Shear Mechanism in Reinforced-Concrete Slabs under Fire Conditions

Link:
Link to publication record in Edinburgh Research Explorer

Document Version:
Publisher's PDF, also known as Version of record

OPEN ACCESS

The Punching Shear Mechanism in Reinforced-Concrete Slabs under Fire Conditions

HOLLY K. M. SMITH, TIM STRATFORD and LUKE BISBY

ABSTRACT

Punching shear transfer at ambient temperature is a complex phenomenon and continues to be the subject of research. The addition of elevated temperature makes the problem of punching shear even more challenging. The shear behavior of reinforced-concrete in fire is dependent upon the degradation of the individual material properties with temperature, their interaction, and the effects of restrained thermal expansion.

This paper reports the experimental findings of fifteen 1400×1400mm slab-column specimens, tested in punching shear at elevated temperatures. A purpose built reaction frame allowed the support conditions to be either restrained or unrestrained. Load was applied to the column stub and the slabs were heated from above using a 960×990mm array of propane gas radiant panels. Instrumentation included strain gauges, thermocouples, displacement transducers and digital cameras for displacement measurement using digital image correlation (DIC).

Clear differences between the behavior of slabs with different support conditions were observed. Unrestrained slabs failed soon after the heating started, whereas the equivalent restrained slabs endured up to two hours of heating. One of the restrained slabs (the most heavily reinforced) went on to fail during cooling. The tests indicated that the diameter of the shear cone does not depend upon the restraint condition, and DIC allowed the crack locations and slab rotation angles to be visualized throughout testing.

INTRODUCTION

The Gretzenbach (Switzerland) car park failure in 2004 raised concerns over the punching shear capacity of flat slabs in fire [1-2]. This unexpected catastrophic failure and loss of life highlighted the need for more understanding of fundamental punching shear mechanisms at elevated temperatures. However, the complexity and cost conducting experimental research has meant only a handful of studies [3-6] have been undertaken.

Holly K. M. Smith, Tim Stratford, Luke Bisby, School of Engineering, The University of Edinburgh, Edinburgh, EH9 3JL, United Kingdom.

To understand the failure mechanisms present in punching shear it is necessary to measure displacements at the shear cone. Traditional displacement measurement techniques are not well suited to elevated temperature testing, and allow only a finite number of measurements to be taken at pre-defined locations. Digital Image Correlation (DIC) is a technique that has been used to measure displacement and strain in structural testing [7]. It uses digital cameras, which can be placed away from any heat source, to take photos throughout a test. An image-processing algorithm allows displacements at any location on the photo to be calculated after the test. Validation of DIC for structural testing is given by Bisby & Take [8], and Gales et al. [9] used DIC for elevated temperature testing.

This paper presents an experimental study of fifteen punching shear reinforced concrete slabs subjected to fire. A brief description of the specimen design, test apparatus, methodology and instrumentation is given. The main focus of the paper is on restraint conditions, failure modes, crack patterns and slab rotation angle.

EXPERIMENTAL TEST SERIES

Specimen Design

Fifteen 1400mm square, slab-column specimens were tested with thicknesses of 50, 75 and 100mm, and a central column stub of 120×120×100mm. The flexural reinforcement was based on the ambient design methods of Guandalini et al. [10], with steel ratios 0, 0.8 and 1.5%. No shear reinforcement was used. Table I gives full details of the slab-column specimens.

TABLE I. SLAB-COLUMN SPECIMENS.

Specimen ID	Fire Scenario	Support Type	Slab Thickness (mm)	Steel Ratio/Diameter (% / mm)	Load Applied During Heating (kN)	Failure Load (kN)
AU50-0.8			50	0.8 / 6	-	54.2
AU75-0.8			75	0.8 / 6	-	101.4
AU100-0	Ambient	Unrestrained	100	0 / -	-	43.8
AU100-0.8			100	0.8 / 6	-	226.3
AU100-1.5			100	1.5 / 8	-	279.7
HU50-0.8			50	0.8 / 6	25.5	55.7[*]
HU75-0.8			75	0.8 / 6	82.8	90.7[*]
HU100-0	Heated	Unrestrained	100	0 / -	30.0	38.9
HU100-0.8			100	0.8 / 6	174.6	174.8
HU100-1.5			100	1.5 / 8	234.0	237.0
HR50-0.8			50	0.8 / 6	26.4	64.4[*]
HR75-0.8			75	0.8 / 6	82.0	115.5[*]
HR100-0	Heated	Restrained	100	0 / -	33.1	82.2[*]
HR100-0.8			100	0.8 / 6	166.5	245.1[*]
HR100-1.5			100	1.5 / 8	232.7	233.2

[*] residual capacity.

Test Arrangement

The slab-column specimens were supported in the reaction frame in an inverted orientation, as shown in Figure 1. A key feature of the frame was that it allowed the boundary support conditions to be either restrained (fixed against in-plane expansion and edge moment, as shown in the right of the figure) or unrestrained (allowed to expand, and free to rotate, as shown in the left of the figure). An array of six radiant panels heated the slabs from above and a hydraulic tension jack loaded the slab through the column stub from below. Full detailed methodology can be found in [11].
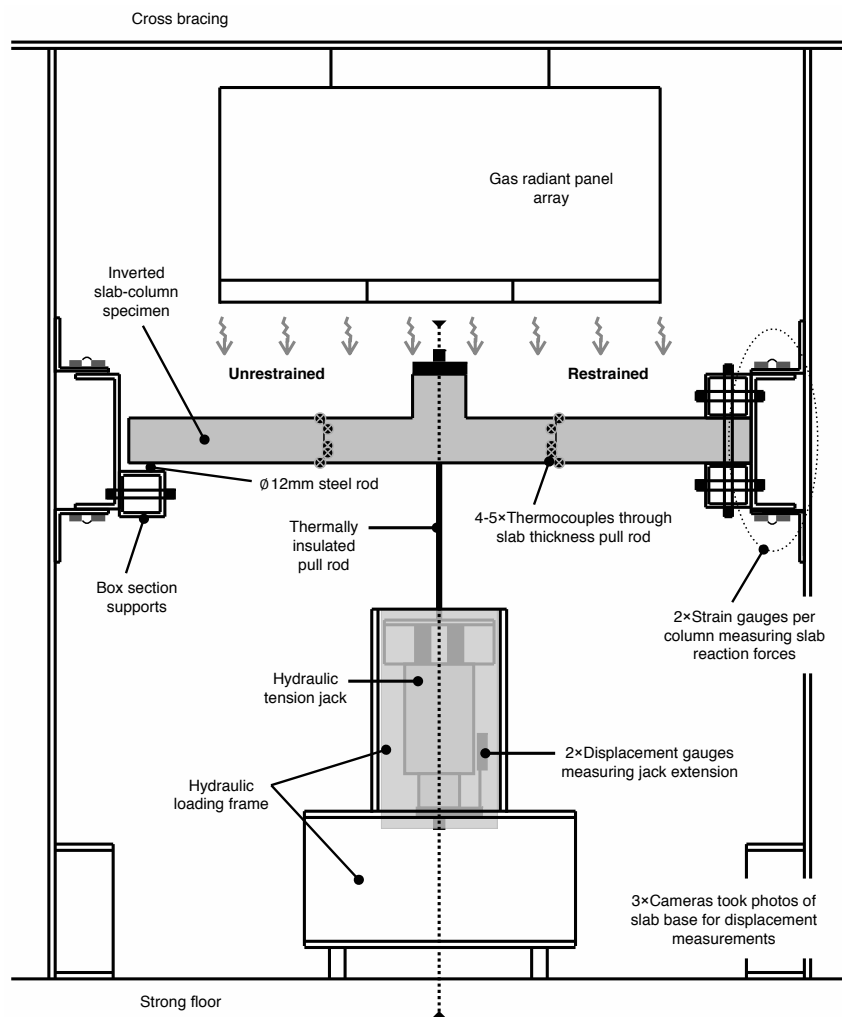

Figure 1. Test setup schematic.

Methodology

Ambient load capacity tests were conducted at a displacement rate of 2mm/min to determine ultimate shear capacity. These ambient test results were used to calibrate a capacity model using Guandalini *et al*. [10], because of the inherent variability in

having a small sample set. This model was then used to calculate the sustained load applied to the heated specimens, which was taken as 70% of the ambient capacity in accordance with Eurocode 2 [12].

In the heated tests, load was applied at the same displacement rate of 2mm/min until the target 70% ambient capacity had been reached. This load was held constant whilst the slabs were heated until failure, or for two hours. These tests did not attempt to follow a standard fire curve; the radiant panels applied a nominal heat flux on the surface of the slab of approximately 50kW/m^2.

The slabs that did not fail after two hours of heating were allowed to cool (with the same sustained load), until the temperatures throughout the depth dropped to below 150°C. Thereafter the applied load was removed at a displacement rate of 2mm/min. Residual tests were conducted on the intact tests the following day.

Instrumentation

The heated slab-column specimens were instrumented with either 12 or 15 thermocouples (depending on the slab thickness). There were three thermocouple trees per slab, located (150mm + d/2) from the column, where d is the slab thickness.

Two conventional displacement transducers were used to record the vertical displacement of the loading rod (at the center of the slab, Figure 1). Three digital SLR cameras were used to record images of the lower unheated surface of the slab, for later analysis using DIC to give the deflected shape of slab. The cameras (2×Canon 650D, 1×Canon 450D) were positioned, out with the reaction frame and looking up at the lower surface of the slab. Images were recorded at 10-second intervals during the loading and heating phases, and 20-second intervals during the cooling phase. The images were post-processed using DIC software, GeoPIV [13] to calculate the vertical slab deflection at any retrospectively chosen location on the lower surface of the slab.

The columns of the reaction frame were instrumented with strain gauges that were intended to measure the boundary reaction in-plane forces and moments due to restrained thermal action (as shown in Figure 1). However, the results from these gauges were not conclusive and are not discussed further in this paper.

RESULTS AND DISCUSSION

The Effect of Restraint Condition on Failure Mode

Figure 2A shows the vertical displacement of the 100mm thick slabs. All of the heated unrestrained specimens tested (HU100-0, HU100-0.8, and HU100-1.5) failed between 4 and 14 minutes into the heating phase. The corresponding heated restrained specimens had a higher capacity and required residual testing. The HR100-1.5 specimen failed during the cooling phase. As far as the authors are aware, this is the first time during a high temperature punching shear test that a specimen has failed during the cooling phase. Figure 2B provides an example of the temperature curves from the HR100-0.8 test. (The depths of the thermocouples are taken from the heated surface of the slab).
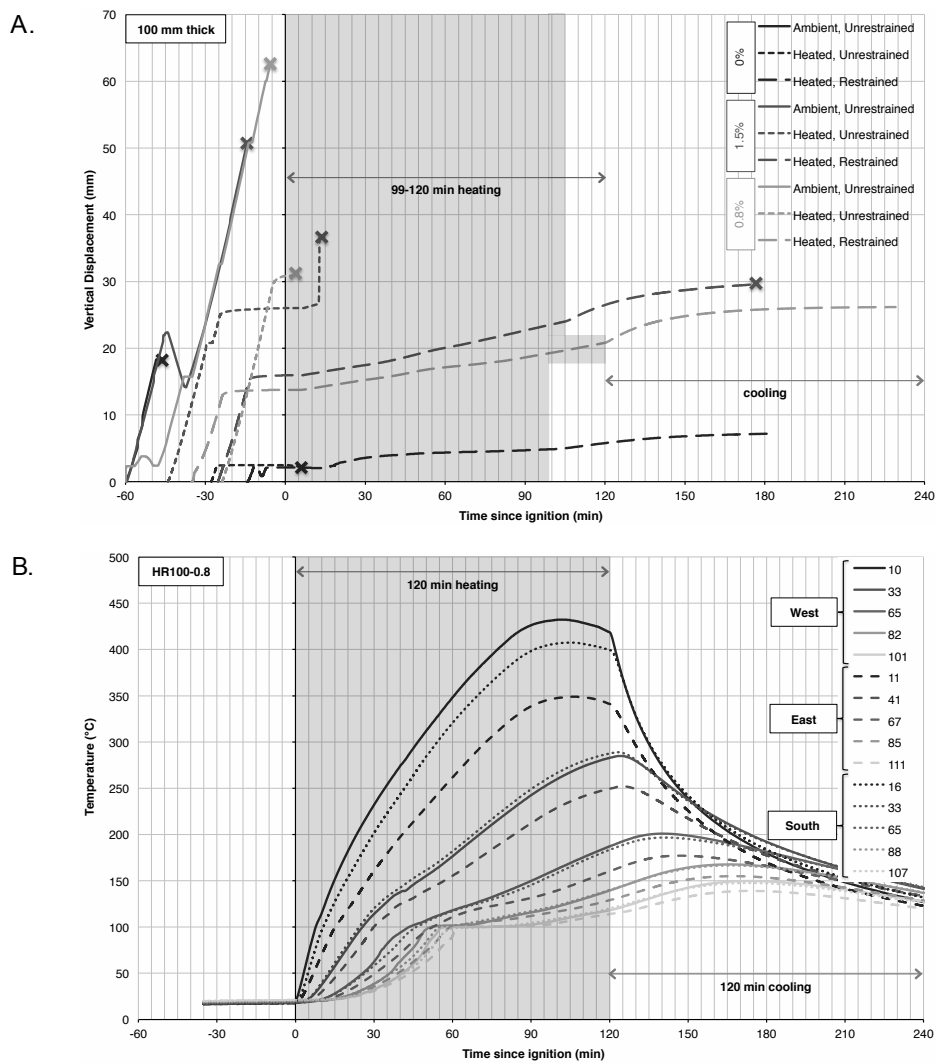
Figure 2. Time history responses: (A) Vertical displacement during the tests on 100mm thick slabs. (B) HR100-0.8 temperature curves at the three thermocouple trees.

Size of the Punching Cone

All the 100mm thick slabs failed in pure shear. The 50mm and 75mm thick slabs failed in flexure-shear mechanisms, and the unreinforced slabs failed in flexure. Figure 3 shows the heated and unheated surface punching shear diameters of all the slabs. The black outlines indicate Eurocode 2 [14] design comparisons for the unheated surface. Eurocode 2 design is conservative because it assumes failure at a smaller load (smaller punching shear diameter) than what we measured experimentally. There is no significant difference in the diameters of the punching shear cones of all the heated 100mm thick slabs, except for the HR100-1.5 slab, which failed during the cooling phase. The similar punching shear cone diameters indicate that the failure mechanisms are the same, despite different reinforcement ratios.
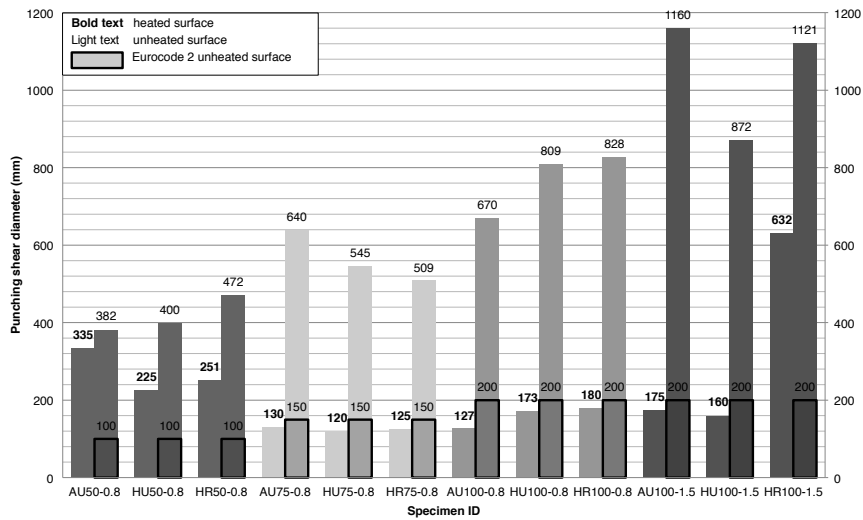
Figure 3. Punching shear cone diameters for heated and unheated surfaces.

Vertical Displacement

The DIC analysis and conventional displacement transducers at the center of the slab were found to be in good agreement, with the DIC measurements slightly less than the displacement transducers, because the latter are affected by loading rod extension and reaction frame movement.

Figures 4 and 5 show the vertical displacement profile across the slab (from DIC) at 10 minute intervals for the 0.8%, 100mm thick slabs. Figure 4 is the restrained slab; Figure 5 is unrestrained. The restrained slab is stiffer and has a maximum vertical displacement of approximately 15mm, whereas the unrestrained slab failed 4 minutes into heating with a maximum vertical displacement of approximately 61mm. The rate of change in vertical displacement across the surface of the slab shows rotation of the slab, and the formation of cracks. As expected, the angle of rotation of the unrestrained slab is much greater than for the restrained slab. The deflection profile in Figure 4 also shows the formation of the punching shear cone during loading.

Note that (as also shown in Figure 2A), the slab displaces away from the heat source and in the direction of loading throughout both the heating (solid line) and cooling (dashed line) phases.
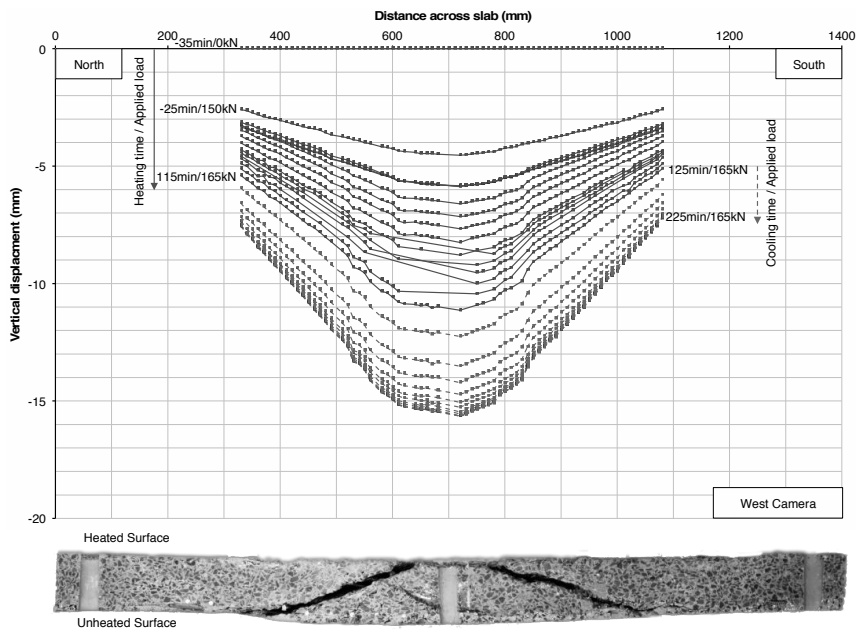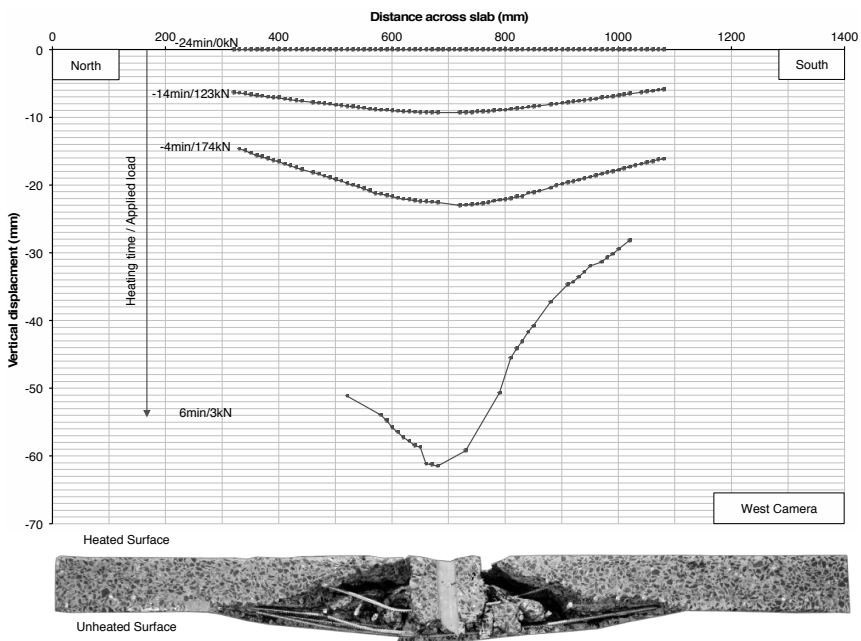
Figure 4. HR100-0.8 vertical displacement.

Figure 5. HU100-0.8 vertical displacement.

CONCLUSION

This paper has presented an experimental study of fifteen slab-column specimens testing in punching shear in fire. The slab-column specimens were tested in a bespoke reaction frame, which allowed the support conditions to be fully restrained or

unrestrained. Clear differences in behavior between these support conditions were observed. The unrestrained 100mm thick specimens failed soon after heating started, whereas the restrained specimens required residual testing. The heavily reinforced, 100mm thick restrained slab failed during cooling with a large diameter punching shear cone.

All the heated 100mm thick slabs had similar diameter shear cones, except for the aforementioned heavily reinforced specimen. This indicates these slabs failed with the same mechanism, and that the punching shear capacity does not depend on the shear cone diameter. Digital image correlation (DIC) was used to measure the vertical displacement of the lower surface of the slab. It allowed crack locations and the formation of the punching shear cone to be clearly visualized for the different support conditions. DIC also permitted the angle of rotation of the slabs to be compared for different support conditions. The rotation of the unrestrained slab was much greater than the corresponding restrained slab.

REFERENCES

1. Muttoni, A., A. Fürst and F. Hunkeler. November 2005. "Deckeneinsturz der tiefgarage am staldenacker in Gretzenbach," Media information from 15 November 2005, Solothurn, Switzerland.
2. Bamonte, P. and R. Felicetti. 2009. "Fire scenario and structural behavior of underground parking lots exposed to fire," presented at the Applications of Structural Fire Engineering conference, February 19-20, 2009.
3. Annerel, E., L. Lu and L. Taerwe. 2013. "Punching shear tests on flat concrete slabs exposed to fire," *Fire Safety Journal*, 57:83–95.
4. Ghoreishi, M., A. Bagchi and M. A. Sultan. 2013. "Review of the punching shear behavior of concrete flat slabs in ambient and elevated temperature," *Journal of Structural Fire Engineering*, 4(4):259-279.
5. Kordina, K. 1997. *Über das Brandverhalten punktgestützter Stahlbetonplatten (On the Fire Behaviour of Reinforced Concrete Flat Slabs)*. Deutscher Ausschuss für Stahlbeton (DAfStb), Berlin (Germany), Heft 479, pp. 106.
6. Salem, H., H. Issa, H. Gheith and A. Farahat. 2012. "Punching shear strength of reinforced concrete flat slabs subjected to fire on their tension sides," *Housing and Building National Research Center Journal*, 8(1):36-46.
7. Hoult, N., A. Take, C. Lee, and M. Dutton. 2013. "Experimental accuracy of two dimensional strain measurements using digital image correlation," Engineering Structures, 46:718-726.
8. Bisby, L. and W. Take. 2009. "Strain localisations in FRP-confined concrete: new insights," *Proceedings of the ICE-Structures and Buildings*, 162(5):301-309.
9. Gales, J. A., L. Bisby and T. Stratford. 2012. "New parameters to describe high-temperature deformation of prestressing steel determined using digitial image correlation," *Structural Engineering International*, 22(4):476-486.
10. Guandalini, S., O. Burdet and A. Muttoni. 2009. "Punching tests of slabs with low reinforcement ratios," *ACI Structural Journal*, 106(10):87-95.
11. Smith, H., T. Stratford and L. Bisby. 2014. "Punching shear of restrained reinforced concrete slabs under fire conditions," presented at the 8th International Conference on Structures in Fire, June 11-13, 2014.
12. Eurocode 2. 2004. *Design of Concrete Structures, Part 1-2: General Rules – Structural Fire Design*. EN 1992-1-2.
13. White D.J., W. A. Take and M. D. Bolton. 2003. "Soil defomation measurement using particle image velocimetry (PIV) and photogrammetry," *Geotechnique*, 53(7):619-631.
14. Eurocode 2. 2004. *Design of Concrete Structures, Part 1-1: General Rules and Rules for Buildings*. EN 1992-1-1.